ADVANCED MATERIALS
www.advmat.de

Cholesteric Liquid Crystal Shells as Enabling Material for Information-Rich Design and Architecture

Mathew Schwartz, Gabriele Lenzini,* Yong Geng, Peter B. Rønne, Peter Y. A. Ryan, and Jan P. F. Lagerwall**

The responsive and dynamic character of liquid crystals (LCs), arising from their ability to self-organize into long-range ordered structures while maintaining fluidity, has given them a role as key enabling materials in the information technology that surrounds us today. Ongoing research hints at future LC-based technologies of entirely different types, for instance by taking advantage of the peculiar behavior of cholesteric liquid crystals (CLCs) subject to curvature. Spherical shells of CLC reflect light omnidirectionally with specific polarization and wavelength, tunable from the UV to the infrared (IR) range, with complex patterns arising when many of them are brought together. Here, these properties are analyzed and explained, and future application opportunities from an interdisciplinary standpoint are discussed. By incorporating arrangements of CLC shells in smart facades or vehicle coatings, or in objects of high value subject to counterfeiting, game-changing future uses might arise in fields spanning information security, design, and architecture. The focus here is on the challenges of a digitized and information-rich future society where humans increasingly rely on technology and share their space with autonomous vehicles, drones, and robots.

1. Introduction

Advanced materials play key roles in technological leaps that affect society. Although the revolution behind our current information age was driven primarily by developments in software and service innovation as well as the concurrent improvements in computing power, wireless communication, and miniaturization, specific functional materials have been critical in delivering the new opportunities to the masses. A striking example is provided by liquid crystals (LCs), without which the flat screens at the heart of the user interfaces of our portable devices would not have been possible. Today liquid crystal display (LCD) technology is highly mature, and other technologies may even provide better solutions for tomorrow's displays, but this does not mean that we have depleted the application potential of liquid crystals. On the contrary, the enormous variety of liquid crystals, in terms of chemical composition as well as physical behavior, opens many avenues to future innovative applications, exploiting different unique aspects of liquid crystals than those utilized in LCDs.

Our society is at the door step to the next technological revolution, as we start to see large-scale deployment of robots and automated vehicles on roads, in city spaces, work places and even homes, and as the environment that we inhabit becomes dynamically modified by augmented reality. Meanwhile, globalization and online shopping have permanently changed national and international markets, with a rapidly growing problem of counterfeiting of valuable products ranging from pharmaceuticals and food products to airplane and automotive components.

These developments will affect us all on a profound level, and just like with previous technological leaps, new, material-based solutions are called for. We can thus expect in the next decade to witness material innovation of entirely new character, driven by challenges that we have not previously encountered and that urgently call for new solutions. At the same time, materials innovation and the resulting availability of novel responsive and dynamic materials are already influencing architecture and design, stimulating radically new thinking with consequent impact on our built environments.[1] It is our objective here to demonstrate that liquid crystals are well fitted to become a key enabling material also in this ongoing revolution, but now applied in contexts very different from that of LCDs. Our hope is that future research on liquid crystalline materials into new directions that are in line with the current societal developments can be stimulated. We focus particularly on smart coatings that carry a wealth of information that can be

Prof. M. Schwartz
College of Architecture and Design
New Jersey Institute of Technology
154 Summit Street, University Heights, Newark, NJ 07102, USA
E-mail: cadop@umich.edu, cadop@njit.edu
Dr. G. Lenzini, Dr. P. B. Rønne, Prof. P. Y. A. Ryan
Interdisciplinary Centre for Security
Reliability and Trust (SnT)
University of Luxembourg
29 Avenue J. F. Kennedy L-1855 Luxembourg, Luxembourg
E-mail: gabriele.lenzini@uni.lu
Dr. Y. Geng, Prof. J. P. F. Lagerwall
Physics and Materials Science Research Unit
University of Luxembourg
162 A Avenue de la Faïencerie 1511 Luxembourg, Luxembourg
E-mail: jan.lagerwall@lcsoftmatter.com, jan.lagerwall@uni.lu
The ORCID identification number(s) for the author(s) of this article can be found under https://doi.org/10.1002/adma.201707382.

DOI: 10.1002/adma.201707382

read out optically thanks to the peculiar behavior arising when cholesteric liquid crystals (CLCs) are molded into the shape of a spherical shell. Their characteristic omnidirectional reflectivity, highly selective and tunable as desired,[2–7] allows the stored information to be visible or invisible to humans as well as to machines. Such coatings may help us confirm the authenticity of a product, reliably identify the user of a service or device, support the navigation of self-driving cars to make them safer, and turn the passive inner and outer facades of buildings into a guiding infrastructure for autonomous vehicles as well as for humans.

Because of the strongly interdisciplinary scope of this article we begin by giving an introduction to CLC shells and their peculiar optical properties in Section 2, together with a brief explanation of how they are produced and how they can be made durable. The remainder of the article aims to give a forward-looking perspective from a security, design, and architecture point of view, in which we critically discuss selected scenarios where we anticipate benefits from CLCs in spherical shape.

2. Cholesteric Liquid Crystal Shells: From Their Production to Their Unique Optical Properties

Liquid crystals are ubiquitous in our lives. They currently find use mainly as the functional material of displays in TVs, computers, tablets, and mobile phones. These devices are rigid and flat, following the traditional approach of enclosing the LC between parallel glass substrates. This paradigm is today being challenged,[8] many researchers investigating spherical LC samples in the form of droplets or shells.[9,10] Both are suspended in an isotropic liquid that is immiscible with the LC, often water, and in case of shells, the LC also surrounds an internal droplet of immiscible liquid, which may or may not be the same as the outer liquid, see **Figure 1**.

While the main focus so far has been on questions of fundamental physics nature, concerning, e.g., the appearance of topological defects and their arrangements, recent reports have also explored potential applications, for instance in sensing,[11,12] in omnidirectional lasing,[3,4] or in security.[5,7,13] With the demonstration that LC shells or droplets can be rendered long-term stable via polymer stabilization[7,13–16] or encapsulation,[6,17] without loss of the unique liquid crystal properties, such applications become technologically viable. In this section, we give the background for these prospects, starting by defining the key concepts.

2.1. Basic Liquid Crystal Terminology

As the name suggests, a liquid crystal combines properties of liquids and crystals,[18] i.e., it flows as a liquid, yet it exhibits macroscopic anisotropic properties as though it were a crystal. LCs carry out this remarkable feat thanks to an anisotropic molecule shape. Typically, they are rod- or disc-shaped, with a well-defined main axis of symmetry. Some common rod-shaped LC-forming molecules (mesogens) are shown in **Figure 2**. The most basic LC phase (and most important from an application

Mathew Schwartz has a BFA and a M.Sc. in architecture with a focus on digital technology from the University of Michigan. He was a research scientist at the Advanced Institutes of Convergence Technology, Seoul National University, in South Korea, focusing on human factors. He is currently an Assistant Professor at NJIT in the College of Architecture and Design. His work, which bridges science and engineering with art and design, focuses on automation in design and the built environment, from integrating autonomous vehicles in buildings to evaluating design based on human factors.

Gabriele Lenzini received M.Sc. in information science and in computer technologies at the University of Pisa (IT), and received his Ph.D. in computer science from the University of Twente (NL) in 2005. After several years of research in companies, in 2010 he joined the University of Luxembourg, where he is now a senior research scientist affiliated with the Interdisciplinary Centre for Security, Reliability and Trust (SnT). His expertise is in system security design and analysis, a subject that he has often approached from an interdisciplinary perspective, teaming computer science up with other disciplines such as biology, social sciences, law, and physics.

Jan Lagerwall received M.Sc. in physics in 1997, Ph.D. in materials science in 2002. He is professor in physics at University of Luxembourg. His research focuses on soft matter physics, chemistry, and materials science, connecting liquid crystals with many other fields, from fiber spinning and microfluidics to art, architecture and security. The motivation ranges from the scientific beauty to the diverse application opportunities arising through cross fertilization with other disciplines. As postdoctoral researcher, he worked with N. Clark (Boulder), G. Heppke (Berlin), and F. Giesselmann (Stuttgart). He previously held group leader positions at Martin Luther University Halle-Wittenberg (Germany) and Seoul National University (Korea).

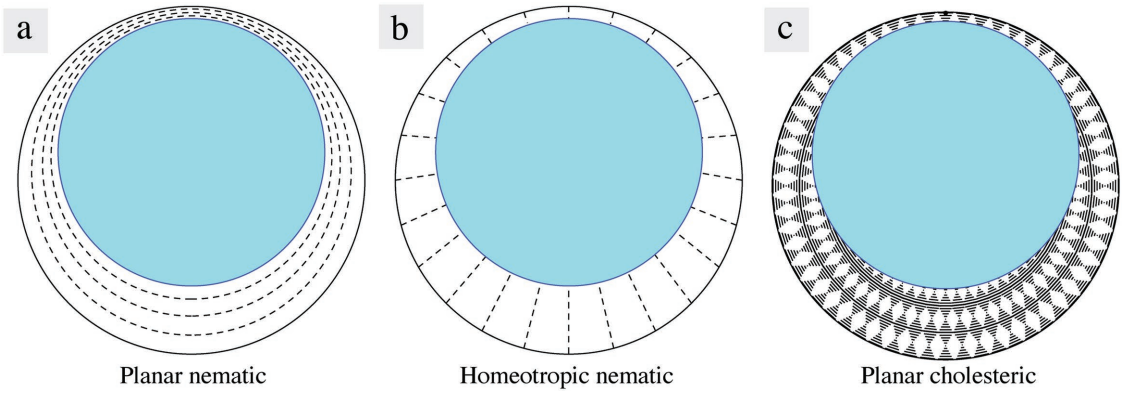

Figure 1. a–c) Schematic cross sections of LC shells of nonchiral nematic type (dashed lines represent director field) (a,b) and chiral nematic type (c) (helix as at the bottom of Figure 2). The blue circle represents the inner isotropic droplet. The shells are drawn asymmetric, as is often the case due to density mismatch between inner phase and LC. Typically, shells are produced with a diameter of 100–300 µm and an average thickness of some 5 µm. c) Adapted with permission.[26] Copyright 2017, Wiley-VCH.

point of view) is called nematic, characterized by the molecules aligning preferentially along a common direction (Figure 2b), termed "director," abbreviated as **n**. This orientational order is not perfect but its long-range extension gives rise to the anisotropic properties of LCs. The most prominent is perhaps birefringence, the director taking the role of optic axis: light experiences a refractive index n_e (extraordinary refractive index) if it is polarized along **n**, that is different from the refractive index n_o (ordinary) for polarization perpendicular to **n**. The magnitude of birefringence is defined as $\Delta n = n_e - n_o$.

If the nematic is cooled, it will typically crystallize into a solid, sometimes first developing intermediate LC phases, and if it is heated above the so-called clearing point, it loses all long-range order and turns into an isotropic liquid. The positional ordering in the nematic phase is only short range, as in a regular isotropic liquid, hence nematics normally flow easily. This fluidity is important since it allows most nematics to be processed as regular liquids. The fluidity also means that the orientation of **n** can easily be changed, for instance by external fields (electric or magnetic), shear flow, or due to contact with certain molecules. Since **n** is the optic axis, a reorientation has strong impact on the visual appearance of the LC, thus control of **n** is key to applications of LCs. The ground state can be controlled by tailored LC boundaries, promoting either *planar* alignment (**n** in the plane of the interface) or *homeotropic* alignment (**n** along the interface normal), see Figure 1a,b. Since spatial variations in **n** come at a free energy penalty, giving nematics a special type of elasticity,[10] the LC transmits the alignment promoted by the interface throughout the sample if it is not thicker than some tens of micrometers. Surface treatments are thus used to control **n** throughout the sample.

2.2. Selective Reflection from Cholesteric Liquid Crystals

The defining characteristic of CLCs (Figure 2d) is that **n** is modulated into a helical superstructure along an axis perpendicular to **n**, with a periodicity p that can be tuned from infinity down to the range of some 100 nm. This helix is a supramolecular expression of the chirality of (at least some of) the molecules forming a phase that locally has nematic order. Cholesterics are therefore also called chiral nematics, abbreviated as N*. Coupled with the birefringence of the phase, with **n** the (local) optic axis, the helix modulates the optical properties periodically. Analogously to the angle and wavelength-selective scattering of X-rays that we know from atomic crystals, this gives rise to selective reflection from CLCs, but in the optical regime, since p is typically on the order of a micrometer.[19,20] The selectively reflected wavelength λ (as measured in air, outside the LC) is governed by Bragg's law adapted to the CLC phase, $m\lambda = \overline{n}\, p\cos\theta$, where m is an integer, $\overline{n}$ is the average refractive index of the CLC, and θ is the angle of incidence (**Figure 3**b). The reflection bandwidth is given by $\Delta\lambda = p\Delta n = p(n_e - n_o)$. With typical visible range values of $\Delta n \approx 0.1$ for common LCs, we get a bandwidth on the order of some tens of nanometers.

Because λ can be in the visible spectrum, CLCs often appear intensely colored, see Figure 3a. This *structural color* is also seen in nature,[20] for instance in peacock feathers or abalone shells. As indicated by Bragg's law, the reflected color shifts to shorter wavelengths with increasing incidence angle θ (Figure 3a,b). A unique feature of CLCs is that the Bragg reflection is elliptically polarized (circularly for $\theta = 0$), with the same handedness as the cholesteric helix. Therefore, if the sample is viewed through a circular polarizer with the opposite handedness, the reflection is largely blocked, see Figure 3c.

2.3. Optical Properties of CLC Shells

When bringing a CLC into spherical shape with planar alignment (thus radial helix), we see the normal incidence ($\lambda_{\theta=0}$) reflection color in a central spot, regardless of the direction in which we observe the sphere, as long as the illumination is along the viewing direction, see **Figure 4**. This is because at the center of the sphere we are always looking along the helix axis. The omnidirectional reflection of a constant wavelength band is a very attractive property of spherical CLCs, in particular for the applications outlined in Section 1, for which the viewing angle dependence of flat CLCs would be detrimental. The striking difference is well illustrated with the macroscopic example by Beltran-Gracia and Parri[21] in Figure 4e.

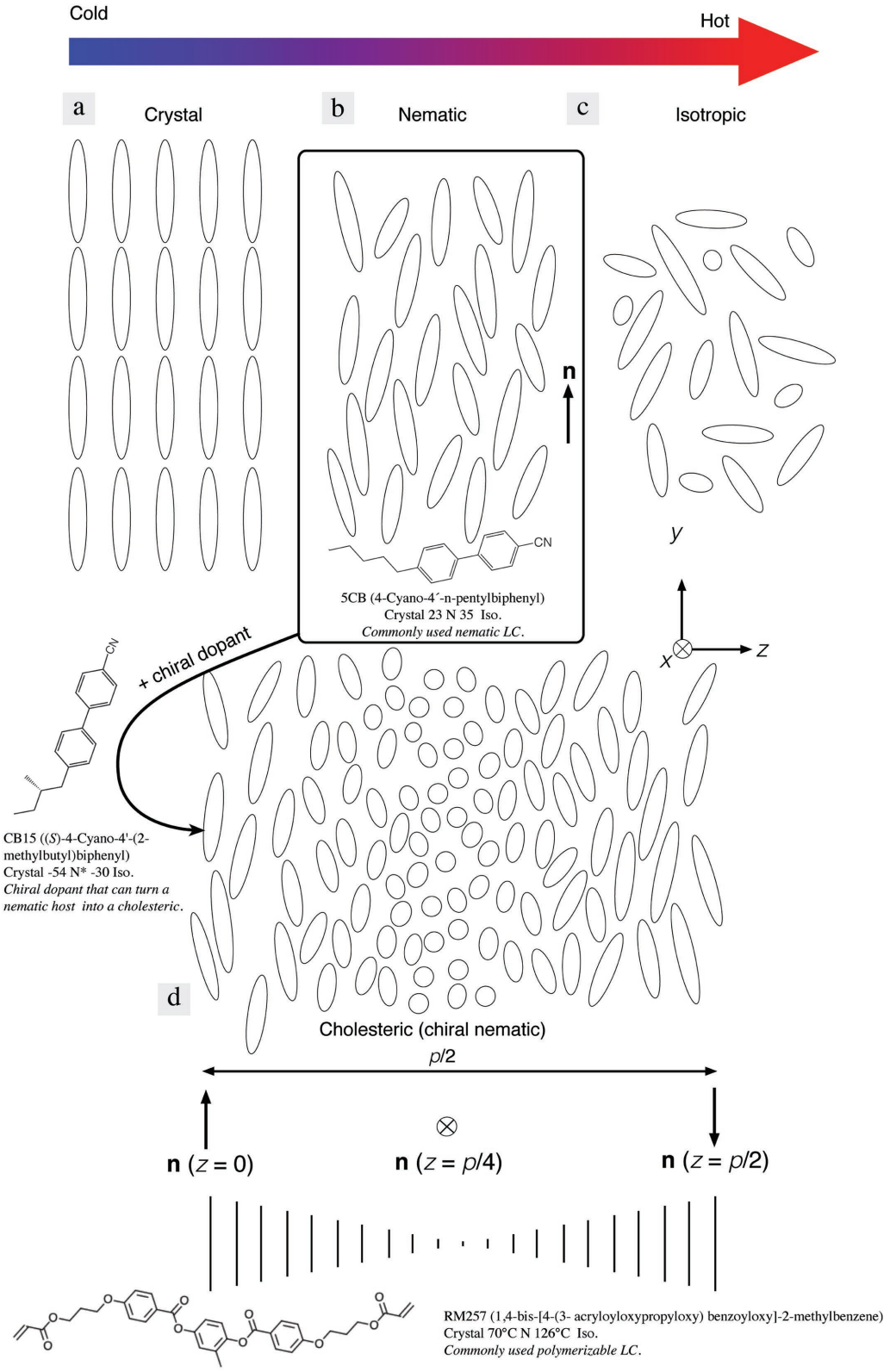

Figure 2. Schematics of the nematic LC phase (b), appearing at intermediate temperatures in a material with rod-shaped molecules (depicted as ellipsoids; shortening represents tilting out of the paper plane), between the crystalline solid (a) and the ordinary isotropic liquid (c). The average molecule orientation is given by the director, **n**. If a chiral dopant is added to a nematic, a cholesteric phase develops (d). The director then rotates around an axis (*z*) perpendicular to **n**. The period of rotation, *p*, is called the pitch. At the bottom a common way of depicting the helix is drawn, used elsewhere here. The commonly used nematic-former 5CB, chiral dopant CB15, and polymerizable (reactive) nematic-former RM257 are shown with chemical structures and phase sequences.

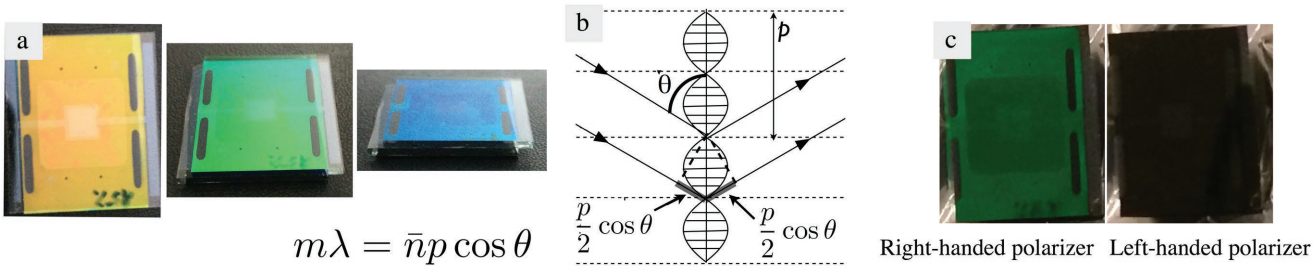

Figure 3. a) A short-pitch CLC reflects visible light in a narrow band around a wavelength λ that depends on the incidence angle θ according to Bragg's law: the reflection wavelength is maximum when viewed head-on (left; the macroscopic sample is about 2 cm wide), and the color is continuously blueshifted as the sample is tilted. b) A schematic explaining the origin of the angle dependence, the cholesteric helix with pitch p drawn vertically. c) Viewing a green-reflecting right-handed CLC through circular polarizers confirms that the reflected light is circularly polarized with the same handedness as the cholesteric helix.

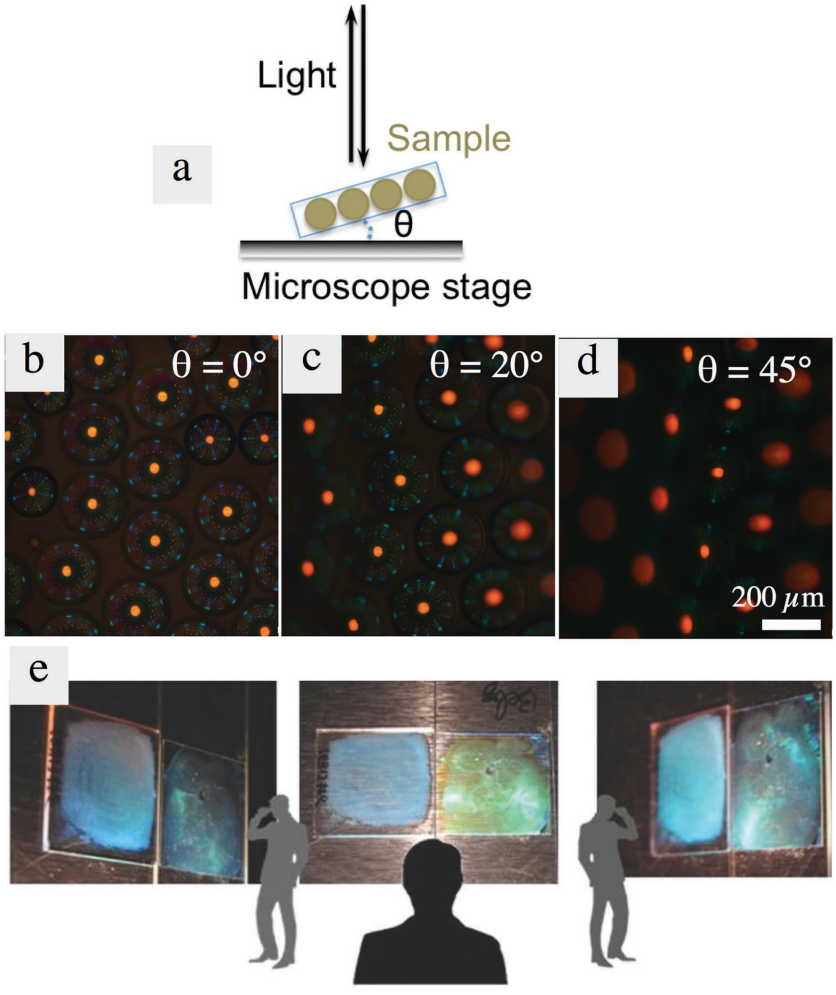

Figure 4. a–d) To confirm the viewing angle-independent color of the central reflection in CLC shells we do polarizing microscopy images in reflection as the sample is tilted at varying angle (a). Every shell in the hexagonally close-packed array of identical CLC shells with $\lambda_{\theta=0} \approx 650$ nm shows a red spot at the center when illuminated and viewed along the same direction (b), corresponding to Bragg reflection for light incidence along the helix axis, and this does not change upon tilting the sample (c,d), although many shells go out of focus. e) Macroscopic demonstration of the viewing-angle-independent color of a film with blue reflecting spheres embedded in a close to index-matched binder (left sample in each photo). For comparison, the angle-dependent blueshift of a flat CLC film that reflects green at $\theta = 0$ is shown to the right in each photo. Reproduced with permission.[21] Copyright 2015, The Royal Society of Chemistry.

The drawback of using spheres is that only a fraction of the sample cross section area gives a visible back reflection, and one might suspect that the overall reflected intensity is therefore too low. Together with Rupp and Drevenšek-Olenik, we recently simulated the reflection patterns from CLC shells,[22] finding that the radius r of the central spot is related to the shell radius R as approximately $r/R \approx 0.34$, the exact number depending on the illumination and observation conditions. The $\lambda_{\theta=0}$ Bragg reflection spot size thus scales linearly with sphere size, keeping a constant area relation $r^2/R^2 \approx 0.34^2 \approx 0.12$. In other words, only 12% of the area is reflective when viewing a single layer of close-packed CLC spheres perpendicular to the sample plane. On the other hand, the reflective area does not decrease upon tilting the sample moderately, in contrast to the apparent overall area of the planar collection of spheres, raising the effective area-normalized reflectivity upon tilting. Moreover, multiple layers of spheres can be stacked on top of each other,[23] and the intensity of the cholesteric reflection is so high that the overall sample appears strongly colored as long as the spheres are small and of good quality, as can be seen in Figure 4e. The blue reflection from the CLC spheres here appears largely continuous on a macroscopic scale, in particular in the two tilted views.

Because we can easily change p by varying the fraction of chiral molecules, we can tune the color of the main reflection across the visible spectrum and beyond.[24] **Figure 5** shows CLC shells with different pitches, corresponding to $\lambda_{\theta=0}$ normal reflection in the near-infrared (most shells in Figure 5b), red (Figure 5d and the two leftmost shells in Figure 5c), or green (the shell on the left in Figure 5b and the four rightmost shells in Figure 5c). We see in this

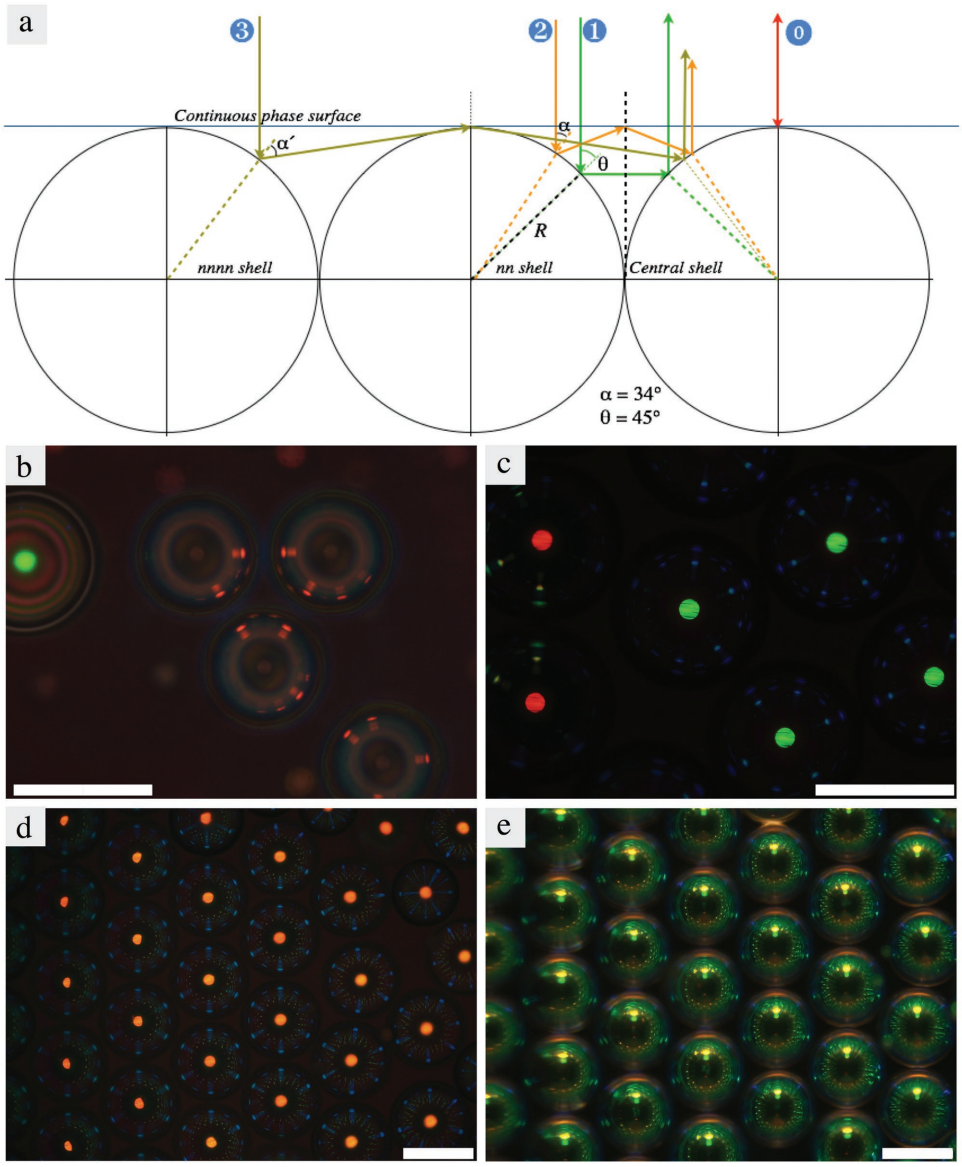

Figure 5. a) When illuminated from above, an array of CLC shells reflects light back up from the top of each shell (path 0) but there will also be reflections directly between shells (path 1) and reflections mediated via TIR events (paths 2 and 3). Because the angle of incidence with respect to the radially aligned cholesteric helix varies, the color of reflection changes according to Bragg's law. The drawing is an evolution of the model originally proposed in ref. [5]. a) Adapted with permission.[5] Copyright 2013, Royal Society of Chemistry. b,c) Reflection polarizing microscopy photos of CLC shells with varying p, yielding $\theta = 0$ reflections ranging from near infrared (most shells in (b)) to green (four shells in (c)) Communication spots appear off-center in the direction of neighbor shells, with a color that depends on the pitches of both involved shells.[7] d,e) A densely packed array of identical shells with red-orange $\lambda_{\theta=0}$ is viewed from above, with illumination that is vertical in (d) but at 45° in (e). The broken symmetry changes locations as well as colors of the reflections. Scale bars: 200 µm.

figure that there are weaker additional spots surrounding the central main reflection, with colors that always correspond to a shorter wavelength than $\overline{n}p$. These spots appear when we have many CLC shells in the same plane, and they arise from photonic cross communication between shells,[5,7] as illustrated in Figure 5a.

A vertical light ray hitting the top of the shell ($\theta = 0$) is Bragg-reflected straight back if it has the wavelength $\lambda = \overline{n}\, p$, giving rise to the central main reflection discussed so far (path 0 in Figure 5a). However, if a vertical ray hits the shell off-center, as in path 1, there will be a reflection for $\theta \neq 0$. Path 1 specifically has $\theta = 45°$, directing the reflected ray horizontally until it hits the neighbor shell, which due to the symmetry reflects the light back to the observer. Bragg's law tells that this reflection path must occur for a shorter wavelength, in this case $\lambda = \overline{n}\, p \cos 45^{\circ}$, which for the normally red reflecting shells ($\lambda_{\theta=0} \approx 650$ nm) on the left in panel (c) is green. This is the origin of the green spots between the two shells, close to their respective periphery. Intershell communication can also take place over longer distance, mediated via total internal reflection (TIR) at the

interface of the continuous phase,[5] as illustrated with paths 2 and 3 in Figure 5a.

For every communication path the reflection angle θ is well defined, hence each path has its own specific wavelength. The result is the pattern of differently colored spots in every shell, at locations determined by the positions of surrounding shells. In reality the incoming light is not strictly vertical, hence we can also have communication between shells with different p.[7] The wavelengths of such communication paths are again different, see Figure 5b,c. With many CLC shells extended over a large area a regular pattern of communication spots appears, see Figure 5d. The generated patterns can be quite complex, uniquely reflecting the particular arrangement of shells and their individual characteristics, and varying with the area of illumination.

Working with shells rather than droplets is advantageous since shells allow faster annealing of defects and polymer stabilization without reduction of optical quality.[7] However, a minimum shell thickness is required in order for the CLC to completely reflect the light that matches the helix. Theoretical considerations show that a thickness on the order of 5–10 pitches is sufficient.[25] In the UV or visible range, this corresponds to just a few micrometers, typical for LC shells. When reflections in the IR range are targeted, the increasing wavelength requires the shells to be correspondingly thicker if we want efficient reflection.

On the other hand, a thickness below the threshold for complete reflection is interesting in its own right if it is only local. As recently shown by Geng et al.,[26] asymmetric CLC shells with thin top and thick bottom allow light to enter the shell interior, where it is multiply internally reflected before again exiting upward through the thin top. The result is multicolored concentric rings, the color of each ring depending on p and the relation between the radius of the ring and the shell,[26] see **Figure 6**. The external reflections giving rise to photonic cross communication are still present, albeit weaker, and by changing the focus either the rings or the cross communication patterns can be accentuated. This gives yet another unique optical feature of CLC shells. Combining the many possible types of reflection patterns and their intimate dependence on shell types and their arrangements, as well as on focus and illumination angle and area, with the practical unclonability of two random shell arrangements, CLC shells emerge as extremely interesting for applications in security,[7,13] as discussed in Section 3.1.1.

Of critical importance for the visibility of the reflections is the minimization of spurious reflections and scattering at the interfaces to the shells, by matching the refractive index of the surrounding medium to $\bar{n}$ for the cholesteric. In an application where many shells are embedded within a binder medium, there will be many interfaces, which will drown any colored reflection if index matching is not achieved. Beltran-Gracia and Parri[21] gave an impressive demonstration of the phenomenon by dispersing polymerized CLC droplet particles of very small size (≈5 µm diameter), with $\bar{n} = 1.59$ and p in the range of colorful reflection, in continuous phases with varying refractive index, see **Figure 7**a. When the particles were suspended in dodecane, with refractive index $n = 1.42$, the selective reflection was impossible to see and the phase appeared white due to scattering. If instead quinoline, with $n = 1.63$, was used for the suspension, the selective reflection color was perfectly visible even in these macroscopic bulk samples. The authors also identified UV-curable binders that provide reasonable index matching, allowing them to prepare the solid films with embedded blue-reflecting spheres shown in Figure 4e. With shells the risk of undesired scattering is even greater since we have to index match both the surrounding matrix and the internal phase. Our preliminary experiments indicate that this can be achieved with polymerized CLC shells and appropriate choice of surrounding phases, as shown in Figure 7c. A complete study of how CLC shells can be embedded in a solid matrix with complete index matching is underway and will be published separately.

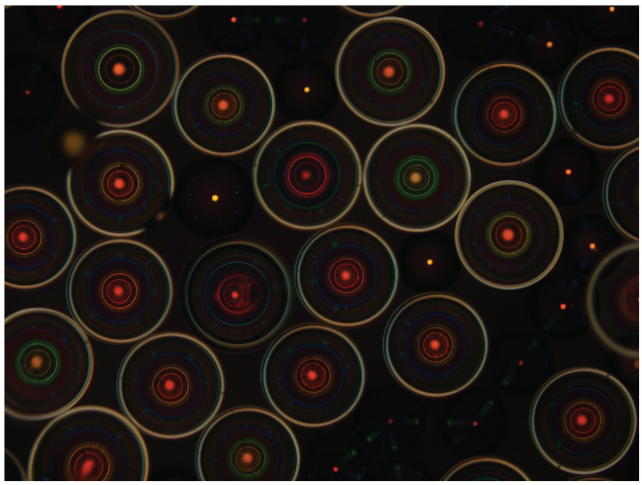

Figure 6. Asymmetric CLC shells with thin top and thick bottom let light into the shell, initiating a sequence of internal reflections that gives rise to concentric rings in each shell, the reflection wavelength depending on ring radius and helix pitch.[26] Here thin-topped shells (about 200 µm in diameter) with $\theta = 0$ reflection in the red and in the yellow, respectively, are mixed at random together with a number of cholesteric droplets. Shell asymmetry with thin top also leads to wavelength-independent total internal reflection between the inner and outer phases, giving rise to the bright white rings.

Comparing Figure 5d,e we see another aspect of CLC shells that has not yet been reported, namely, that the reflection pattern changes substantially if the angle of illumination no longer coincides with the observation direction. In both photos an array of normally red-reflecting shells ($\lambda_{\theta=0} \approx 650$ nm) illuminated by white light is observed from above in the polarizing microscope. However, while the shells are illuminated from above by the microscope lamp in Figure 5d, they are illuminated by an external light source in Figure 5e, hitting the shells at an angle of about 45°. The central reflection spot disappears and instead a dual set of direct reflection spots appears, shifted off-center in the direction of the lamp. Following Bragg's law, the color is blueshifted as a result of the increased angle θ. Also the communication spots change, the smallest ones close to the center exhibiting an azimuthal variation in both color and distance from the shell center. The peripheral spots change color and the symmetry given by the hexagonally close-packed arrangement is broken. A complete elucidation of the complex response to changes in illumination direction is an important challenge for the future.

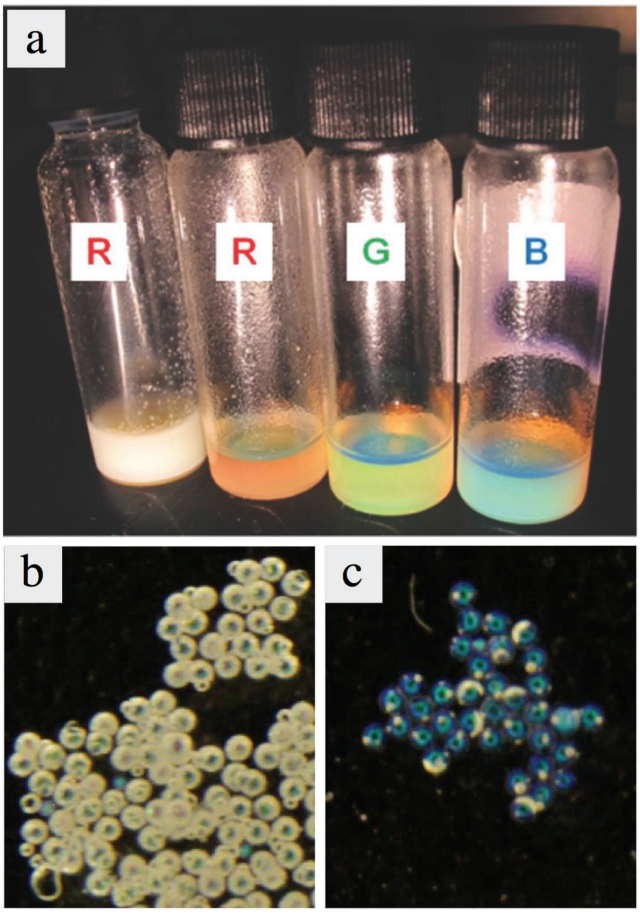

Figure 7. a) The importance of index matching between CLC spheres and the surrounding medium is demonstrated by having red-reflecting CLC droplets in a nonindex matched continuous phase (left vial) and red-, green- and blue-reflecting spheres in a near index-matched continuous phase (remaining three vials). Reproduced with permission.[21] Copyright 2015, The Royal Society of Chemistry. With CLC shells (b,c), the index matching gets even more challenging, as inside as well as outside phases must have similar refractive index to the CLC. Photo (b) shows the macroscopic appearance of a group of polymerized CLC shells with $\lambda_{\theta=0} \approx$ 500 nm (each is about 200 µm in diameter) that have not been index matched to the surrounding phases, showing essentially no reflection color and instead just a strong broad spectrum light scattering. In panel (c), the same types of shells are filled and surrounded by index matching materials, clearly revealing the reflection color and giving scattering only in small areas with imperfections. Because the illumination is lateral inclined rather than vertical, the central green reflection is not visible, and instead a blue ring is detected in each shell (see Figure 5).

2.3.1. Oil-Based versus Renewable CLCs from Plants or Animals

While the majority of today's LC materials are oil-based, there is a strong and growing interest in renewably produced CLCs, derived from biological cellulose or chitin sources.[27] Both cellulose and chitin are chiral, and protocols have been established for producing crystalline needle-like particles from natural sources such as wood or cotton (cellulose) or crustacean shells (chitin). The cellulose case is the most widely studied, and the term cellulose nanocrystals (CNCs) has been established for these nanorods. When suspended at an appropriate concentration in water, the particles organize with long-range orientational order along a common direction **n** thanks to the rod-like shape. Moreover, because of the chirality, **n** rotates helicoidally. The phase is thus a cholesteric LC and its reflection can be tuned from IR to visible by changing the cellulose/chitin concentration. The bioderived CLCs are interesting not only because their sustainable production opens for low-cost photonic materials made from waste products like seafood trash, but also because they should be more resistant to continuous UV light exposure from the Sun than many oil-based cholesterics, where lifetime may be an issue.

An even better approach to ensure long life time, which can also be made insensitive to wind and weather, is to template inorganic materials from the CLC. This technique has been pioneered by MacLachlan and co-workers, using cellulose-derived CLCs to produce structurally colored glass,[28] titanium dioxide,[29] and other inorganics. While such replicas lose the intrinsic responsiveness of the original CLC, they would be very interesting for passive coatings containing omnidirectionally reflecting CLC-templated shells. Additionally, cellulose derivatives like hydroxypropylcellulose are interesting[30] as they can develop selectively reflecting cholesteric phases in various solvents or on their own at high temperatures.

2.4. Microfluidic Production of LC Shells

To produce LC shells with high monodispersity in diameter and thickness, a suitable method is capillary microfluidics. All protocols are typically evolutions of the original procedure for making isotropic multiple emulsions in a microfluidic setup presented by Utada et al. in 2005.[31] Two cylindrical capillaries are inserted from two sides into a capillary with square cross section, the inner side length of which is equal to the outer diameter of the cylindrical capillaries. Both cylindrical capillaries are tapered toward the inside, see **Figure 8**. The inner isotropic phase, which will form the droplet holding up the LC shell, is pumped through one of them, and the LC (immiscible with the inner phase) is pumped in the same direction through the corners of the square capillary surrounding the cylindrical one.

From the other side of the square capillary the outer phase (also immiscible with the LC) is pumped in the opposite direction, in the corners surrounding the other cylindrical capillary. The latter functions as collection tube for the final double

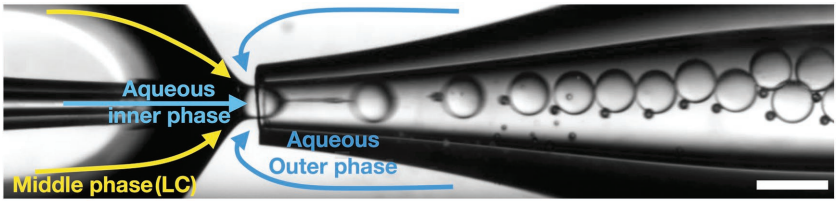

Figure 8. Liquid crystal shell production using a coaxial glass capillary microfluidic setup. The shells are about 130 µm in diameter and less than 3 µm in thickness (scale bar: 200 µm). Image provided by and reproduced with permission of J. Noh.

emulsion. At the junction where the LC with coflowing inner fluid meets the counterflowing outer phase, the former stream is flow-focused into the orifice of the collection tube. The composite stream breaks up due to the Rayleigh–Plateau instability, giving rise to composite droplets with the inner isotropic phase at the core, surrounded by a thin layer of LC, and suspended in the outer isotropic phase. The production is fast, ≈100 shells s^{-1}, a rate that could be further boosted by employing multiple sets in parallel. In Figure 8, both the inner and outer phases are water-based, containing also glycerol and poly(vinyl alcohol) (PVA) as stabilizer (see below).

The key parameters controlling shell diameter and thickness are the sizes of the orifices of the two cylindrical capillaries and the flow rates and viscosities of all involved liquids.[31,32] Successful production requires well-centered capillary tips and cleanly cut orifices, hence the capillaries are normally tapered in a professional pipette puller and the molten end then cut open with a microforge. With such instruments, orifice diameters in the range of 50 µm can be realized with high reproducibility, allowing reliable production of shells with diameter on the order of 100 µm and thickness on the order of a micrometer. Because the emphasis has so far been on minimization of shell size there are no reports on upper size limits, but in some experiments in our labs we have produced shells with diameter on the order of 1 mm. There is no reason to believe that this is an upper limit.

2.4.1. Controlling Liquid Crystal Alignment in Shells

In order to prevent the shells from collapsing, surface-active stabilizers must be added to the isotropic phase(s). The choice of stabilizer is extremely important, not only because it is critical for allowing the production of shells and giving them reasonable lifetime, but also because the stabilizers can drastically influence the alignment of **n** at the interface(s) to the surrounding phase(s). They may even have a subtle influence on the phase sequence.[33] Water typically induces planar alignment of thermotropic LCs,[34] hence the planar alignment, desired for the CLC shells considered here, is achieved by using an aqueous surrounding phase and a stabilizer that does not itself influence **n**, such as PVA.

2.4.2. Making Liquid Crystal Shells Mechanically Robust

Liquid crystal shells are delicate. To render them long-term stable, it is important to either transform the LC state into a solid or to shield it. While the latter may be done by polymerizing the continuous phase, as in polymer-dispersed liquid crystals,[35] the polymerization-induced shrinkage of the continuous phase is likely to burst the shells, and the procedure gives little freedom for postprocessing. Better is to polymerize the LC itself or a thin protective layer around it. The latter option was explored with success for the case of CLC droplets by Kim and co-workers,[6,17] preparing the droplets with a thin outer shell of a reactive isotropic liquid, photocured after production.

If the LC itself contains reactive mesogens, e.g., with acrylate end groups as in the commonly employed RM257 (Figure 2), the polymerization can be done within the LC shell.[7,36] If all mesogens are reactive, a glassy solid results which, in the best case, retains the structure of the LC precursor. Also CLC droplets can be polymerized successfully in this way if they are very small, like the ≈5 µm droplets turned into particles by Belgran-Gracia and Parri.[21] However, if droplets on the order of 100 µm are desired, some loss of alignment often results.[16]

Better results can then be achieved with shells, thanks to the confinement of the CLC between inner and outer phases that both impose planar alignment. With 20% RM257 mixed into a CLC mixture of unreactive components, Geng et al. polymer stabilized CLC shells with minimum loss of order. Yet the stabilization gave sufficient mechanical stability for the shells to support substantial compression without rupture.[7] Noh et al. used an even smaller amount to polymer stabilize nematic and smectic shells, finding that the result depends sensitively on the mixture composition and the conditions under which polymerization is initiated.[15] With optimum conditions, a major increase in shell stability could be achieved even while the LC remained responsive enough to go through phase transitions.

3. Future Application Scenarios for Cholesteric Shells

Having introduced the characteristic optical properties of CLC shells and the basics of their production, we now turn to exploring how these shells could be utilized to create innovative materials with unique functionalities. Because our focus is on advanced materials that fill expected emerging needs of our future societies, and which can inspire *users* of the materials to develop innovative solutions in their own fields, we take an analytical perspective from a broad functional design and architecture point of view. This allows us to identify some very exciting potential application areas of coatings that are enhanced by the behavior of incorporated CLC shells.

In design, architecture, and construction, materials and their properties are utilized in various ways depending on the scale, influencing the interactions between occupant and space on a multitude of levels. Relevant scales span from finger-sized to entire cityscapes. For instance, the properties of steel can be leveraged for the strength of holding up buildings, while a thermostat may use the steel as a tiny spring. Similarly, by designing composite materials strategically, a material used for decades can be endowed with new properties thanks to functional components embedded within. Examples of such new performing building materials range from concrete with glass fiber reinforcement, with enhanced structural properties, to glass sandwiched with aerogels, improving acoustical and thermal insulation. Aksamija[1] identify additional advanced materials that have been demonstrated within architecture, such as electrochromics, shape-memory alloys, self-healing materials, phase-change materials, photovoltaics, and thermoelectrics. Learning from previous and current applications of innovative materials, we conclude that any consideration in the way new advanced materials—including those utilizing CLC shells—can be utilized and affect designed spaces should include a wide variety of purposes at different scales.

Before going through the various application scenarios that we consider in this vein, we identify three main functionality classes, defined by the relevant CLC shell properties that they exploit:

1. Dynamic complex pattern generators from clusters of cholesteric shells.
2. Sensors based on soft polymer-stabilized CLC shells.
3. Omnidirectional CLC shell back reflectors.

In the first two classes, we are dealing with minute to small scales, whereas the third is considered mainly on large and intermediate scales.

3.1. Human Scale and Below

Considering first the scale of a human, a person's physical interaction (primarily touch and vision) with an object and the materials from which it is made is vital. On this scale and below, the subtle features from photonic cross communication between CLC shells become realistic to exploit. Because any deformation affects the communication paths and is thus immediately amplified into changes to the generated patterns, a pressure sensor with high location and pressure resolution might be developed, of particular interest for human scale robotics, as described in Section 3.1.2. The sensitivity of the CLC pitch to various chemical influences could also be used in small-scale chemical detectors incorporated in objects we manipulate in our daily lives, for instance when eating. But before discussing these future possibilities, we will describe a slightly further developed application scenario, namely in security, as tags that would uniquely identify a person or an object.

3.1.1. Product Authentication and Anti-Counterfeiting

Authentication of digital and physical artifacts is a central concept in *security engineering*. Guaranteeing the authenticity of items ranging from *objets d'art* to fashion items has great commercial importance, but it can also have health and safety implications to combat counterfeit medications and spare parts. The counterfeiting of goods can affect practically any marketable item[37] and has been boosted by online commerce where products can be sold and distributed with almost no regulations and controls. In 2015, a white paper by the Europol and the Office for Harmonization in the Internal Market[38] estimated on the basis of reported incidents—probably representing just the tip of the iceberg—about 36 million recognized fake articles in the European Union. Among them are luxury goods, foods and drinks, cosmetics and medicines, pesticides,[39] digital storage media (SD cards), and parts for airplanes and cars.[40]

In this context, CLC shells may come to play a very important role, potentially forming the basis of a game-changing material for authentication. In fact, the optical features of clusters of CLC shells suggest considerable potential in security,[7,13] allowing the production of a physical identifier tag that is effectively unclonable as a result of the manufacturing process, naturally tamper-evident and hard to simulate due to the complexity of the generated patterns. Our envisaged identifier tag would typically be created by dispensing a suspension of polymerized or polymer-stabilized CLC shells of different types (different pitch, handedness, radius, thickness, etc.) in an index matching continuous phase that can rapidly be solidified, e.g., by UV curing. Since the particular arrangement of shells realized through this procedure is intrinsically random, and thereby the optical patterns produced upon illumination, the details of the patterns from a certain tag cannot be predicted prior to its production. Moreover, by quickly solidifying the continuous phase, ideally while the suspension is still flowing, the shells will not have reached their equilibrium arrangement. Such a frozen-in dynamic arrangement would result in even greater diversity, due to the very fact that it is nonequilibrium, hence each disposition of CLC shells produced in this way will be physically unique, unclonable, and unpredictable for all practical purposes. Not even the manufacturer of an identifier tag utilizing CLC shells in this way could reproduce it.

The envisaged tags would have another key strength for secure authentication: a virtually unbounded space of challenge–response pairs. Unlike simple code-carrying tags, and thanks to the CLC shell response to luminous stimuli, authentication here would not be carried out by revealing a stored secret, but rather by reproducing a complex behavior which is intrinsically bound to physical features that are fixed at production time. For these reasons CLC-shell-based identifiers emerge as members of a category of materials known as physical unclonable functions (PUFs).[41] **Figure 9** shows how the generated *optical pattern* of even a very simple regular arrangement of identical CLC shells changes with illumination area (Figure 9a–d), with focus (Figure 9e–h), or by switching to transmission between crossed polarizers (Figure 9i), or with a $\lambda/4$ phase plate inserted (Figure 9j). Add to this variety of textures the options of tilting the sample (Figures 4 and 7), using oblique incidence illumination (Figure 5e), using circular polarized light for illumination, combining thick- and thin-topped asymmetric shells (Figure 6), or incorporating a temperature-responsive CLC core[14] inside some of the shells, it becomes apparent that the number of challenge–response combinations is truly enormous.

The potential application in authentication is not limited to valuable objects that are subject to counterfeiting. CLC shells may also play a powerful role in multifactor authentication of persons, in particular in strengthening user authentication tokens (*something I have* factors). Such tokens would be complementary to biometrics (*something I am* factors) and, in contrast to biometrics, would be disposable and renewable.

Each CLC-shell-based identifier is capable to respond uniquely to different stimuli, that is, to any precise configuration of illumination (e.g., incidence angle, location, aperture, and polarization) and imaging (focus, location, angle, ...), potentially also variations in temperature or application of electric or magnetic fields. The responses are the various patterns that result at each condition of stimulation, patterns that we estimate to be complex enough to be unfeasible to simulate. Such a rich set of responses can be used to build protocols for authentication where, underpinned by proper cryptographic tools, the verifier and the identifier play a challenge–response game where authenticity is confirmed only when all the

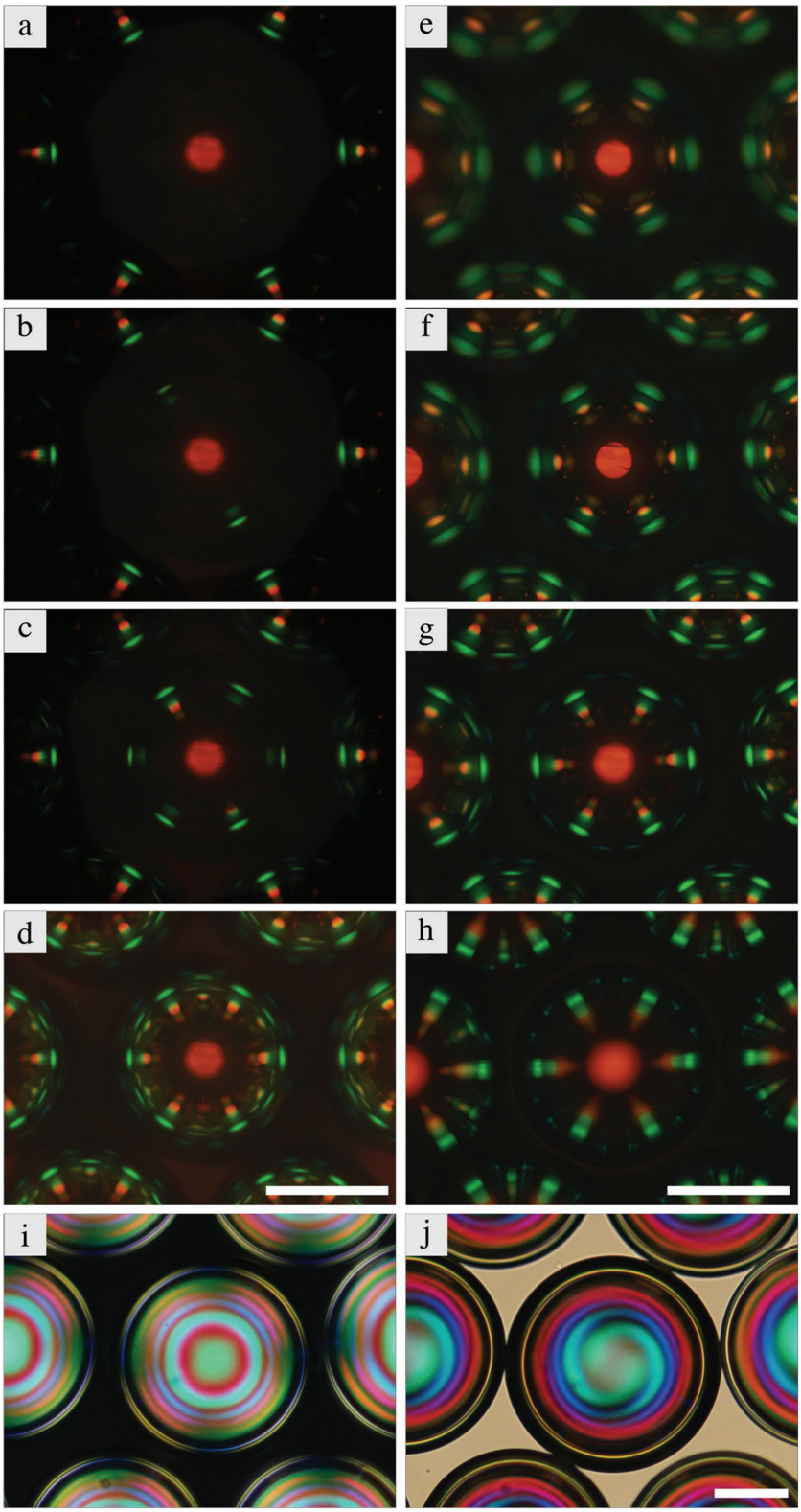

Figure 9. Polarizing microscopy textures of hexagonally close-packed arrays of normally red-reflecting shells observed in reflection a–h) and in transmission i,j). From (a)–(d) the illuminated area of the same sample is continuously expanded from the center, in (e)–(h) another sample of the same type imaged with the focus varying from top (e) to bottom (h). The shells in (i) belong to a third sample, viewed in transmission between crossed polarizers, and in (j) a $\lambda/4$ plate has been inserted. Scale bars are 100 µm.

expected answers are correctly delivered in response to randomly selected challenges.

Our arrangements of CLC shells would offer two advantages compared to previously proposed PUFs, e.g., in microchips[42] and paper manufacturing.[43] First, they provide tamper evidence against any attempt of physical forgery since removing them will ruin their structure and invalidate the challenge–response behavior.[7] Second, CLC-shell-based tags have an unprecedented range of applicability. The shells would be integrated in a matrix that can be made of different materials, and by tuning *p*, the shells could be made visible or invisible, as desired. This enables the incorporation of a cluster of CLC shells in objects directly at manufacturing time. Such deep integration into the object to be authenticated creates an unbreakable bond between a tag and its host, hence the object effectively becomes its own tag. This opens for applications in fields where currently there is no efficient defense against fraud, like in counterfeit pharmaceuticals. Most pills hold the active substance in a so-called excipient, typically made from a cellulose derivative such as hypromellose or hydroxypropylcellulose, or from collagen. Interestingly, all these polymers can generate cholesteric LC phases,[30,44] hence an opportunity arises to make food-grade CLC-shell-based tags, allowing authentication even of individual pills.

There are still many technical details to be resolved before this innovative technique could become of common use, and it is our hope that the presentation of the concept can stimulate further research in this direction. Depending on the type of object to be authenticated, the chemistry may need to be adapted to the target environment, e.g., using cellulose-based CLCs for authentication of pharmaceuticals or inorganic materials if long-term exposure to sun light is expected. Also the matrix material needs tailoring, ensuring index matching and the possibility of rapid solidification while being compatible with the particular target environment. While the microfluidic production can be parallelized for increased production rate, alternative production methods may be better adapted to upscaling. There are also important challenges on the computer science side. In order to extract the identifying features of a CLC shell bundle from its colored patterns, we need precise and efficient image processing algorithms and technique of information extraction that are robust but still capable of maximizing the unpredictability and unsimulability that make CLC-shell-based patterns so interesting for security.

3.1.2. Small-Scale Sensing Enabled by CLC Spheres

Moving from security to robotics, material feedback is a key area of exploration, with tactile feeling being an important challenge. While humans are very capable of sensing different textures and minute differences in height, the accuracy of a robotic limb using current and conventional design to detect these changes is limited. A material that is able to give the robot localized pressure-sensitive feedback from physical contact could then be extended to give even more detailed information than can be sensed by a person. Likewise, small variations in temperature or humidity could be detected by a robot equipped with adequate responsive materials. While a spectrum-resolving heat camera may work in many situations, the cost, weight, and field of view being limited to the position and orientation of the camera make it ill suited for a generalized application. Likewise, CLC shells allow for a more passive approach, reducing power consumption on mobile robotics.

Polymer-stabilized CLC shells that still retain their softness could be used as high spatial resolution pressure sensors. As demonstrated by Geng et al.,[7] a CLC shell with about 20% polymer component is sufficiently stable mechanically to sustain considerable compression, yet, as the shell is compressed, the optical signature is continuously changed, see **Figure 10**. By illuminating an array of such shells distributed within a soft rubber skin matrix (e.g., made of silicone rubber) from behind with a white light-emitting diode (LED) and monitoring the reflection pattern, a robot could get a high-resolution (in space as well as in pressure) pressure-sensing capability at its finger tips. Even small relative deformations give strong changes in the optical pattern. Since the shells are on the order of only 150 µm in diameter, an accurate sensing function would be expected.

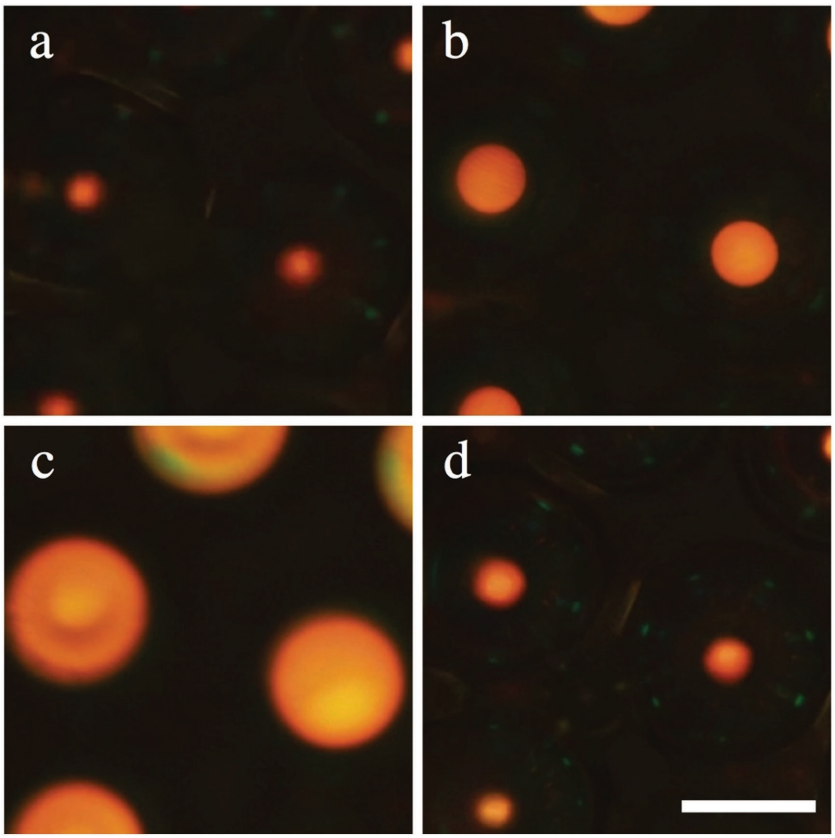

Figure 10. Polymer-stabilized short-pitch CLC shells sustain strong mechanical pressure without rupture, changing their optical signature continuously. Panel (a) shows the undeformed shells whereas they in (b) and (c) are subject to increasing compression. The photonic cross communication pattern is first distorted and then disappears as the compression increases. The central $\theta = 0$ reflection spot increases continuously in diameter and some variation in reflection color is also seen. These strong changes in optical appearance in response to compression could be used for spatially resolved pressure sensing. Panel (d) shows the shells after pressure release, returning to their initial state with the original optical properties intact. Scale bar: 100 µm. Reproduced under the terms of the Creative Commons Attribution 4.0 International License.[7] Copyright 2016, The Authors, published by Springer Nature. This article also contains a movie of the full compression cycle.

In safety, visibly detecting hot spots or other dangerous elements can prevent injury. The responsivity of CLCs to temperature, changing their color upon heating or cooling, could be highly useful in this respect. Likewise, alerting about the presence of invisible danger elements such as clear but toxic gases or liquids are prime targets for material feedback. Past designs show this well, such as cup materials that change color when in contact with gamma-hydroxybutyric acid (GHB, known as the date rape drug) to let people know that their drink has been tampered with. Similarly, a normally transparent coating applied to silverware, which changes to a colored state if exposed to specific allergens (such as seafood or certain nuts), could save lives.

Liquid crystals may be interesting in this context, as a number of studies have demonstrated their ability to sense specific chemicals in their environment. The spherical shape of shells here provides a critical advantage as the response becomes unambiguous thanks to the loss of viewing angle sensitivity (see Figure 4). For detecting acids like GHB (or potential basic additives) pH sensing is useful. This was recently demonstrated with CLC shells by Jang and Park.[11] The authors used a block copolymer with one liquid crystalline and one poly(acrylic acid) block as outer shell stabilizer, resulting in an alignment change from uniformly planar alignment (radial helix, hence visible selective reflection) at pH < 7, to hybrid alignment (planar inside, homeotropic outside), giving a patterned and much weaker reflection, for pH > 7. These shells would need to be lightly polymer-stabilized,[15] and/or the block copolymer stabilizer might be (partially) crosslinked, in order to make them durable enough for using in a sensor strip that could detect abnormal changes to pH. By developing other block copolymers for stabilizing the shell and controlling the LC alignment, shells optimized for detecting various allergens might be developed.

Han et al. demonstrated oxygen and carbon dioxide sensing, respectively, using CLC mixtures with appropriate chiral dopants.[45] Upon exposure to the analyte the helix pitch changes, with a consequent change of color that can easily be detected by the naked eye. Abbott and co-workers used the interaction between the commonly employed LC material 5CB and aluminum perchlorate salts to realize an anchoring transition in the case of exposure to dimethyl methylphosphonate (DMMP), which is a simulant for chemical warfare agents like sarin.[46] While this sensor, based on the reorientation of a nonchiral nematic, required observation between crossed polarizers, the principle of detection is based on an analyte-triggered change of alignment. This should be applicable also to a short-pitch CLC, allowing a color changing sensor.[47] In our own research we have demonstrated that LCs incorporated in fibers can sensitively detect volatile organic compounds such as toluene.[48] Although gas sensing with LC shells has not yet been demonstrated, the fact that the encapsulation in the polymer fiber sheath does not prevent access of the analyte to the LC is a promising indication that the gas sensing concept can be transferred also to LC shells for omnidirectionally visible response.

3.2. The Scale of Cities and Their Buildings

On a much larger scale, there are fascinating opportunities for applying coatings with incorporated CLC shells. This is interesting both because of the unique functionality provided by the shells and thanks to the low cost at which the coatings could be produced. It might seem surprising that we consider the application of minute objects like microfluidic-produced CLC shells on scale as large as that of cities, but this is motivated by two important characteristics of these shells and the way they are made. First, the fast and continuous microfluidic production, and the autonomous generation of the functional structures by liquid crystal self-organization, allows for rapid production of a large number of identical responsive shells, which can then be brought together (or mixed with shells with slightly different properties) to cover macroscopic areas.[6,7,21,49] Since we are dealing with coatings incorporating the shells, we only need to cover 2D areas, not fill up 3D bulk. Second, since CLCs respond autonomously to light, temperature, chemical variations in the atmosphere, etc., by selectively reflecting certain wavelengths and polarizations, possibly changing in response to the stimuli, there is no need for wiring or tubing to the individual components, in contrast to devices driven by electricity or combustible fuel. Thanks to this autonomy it becomes feasible to create large-scale functional elements, with sufficient size to perform relevant architectural or design functions, that consist of thousands of tiny CLC shells acting in concert. This is not unlike the overall construction of a building in which small parts are aggregated to build a larger, cohesive, structure.

Major application areas of advanced new materials on the city scale are transportation and locomotion. Currently, indiscriminate retroreflection technology using glass spheres is used on road signs for improved visibility. Street signs and building numbers are also used to help in navigation of both vehicles and pedestrians. While more information to a user in many cases is desirable, visual noise can increase the time it takes to find relevant information.[50] Special or localized information to a particular agent in the space is often provided through electronic communication such as WiFi. While this solution has been useful for general information, accurate localization and contextual information is difficult to convey. Instead of adding more signage or other information within the visible wavelength window, a spectrum guide could be used for separating information.

CLCs can provide such spectral data separation, analogous to radio channels being separated by their frequencies, with the further possibility of separation by polarization. By bringing them into shells, we additionally profit from omnidirectional reflection at a wavelength that is independent of viewing angle, of utmost importance for communication along directions that are not known beforehand. If we tune the CLC reflection to the infrared range, an information-rich landscape would arise that is visible only to machines designed to communicate in this part of the optical spectrum, while additional information overload on humans is avoided.

Autonomous vehicles are a prime example of why signage and information about the city would benefit from spectrally separated optical communication channels that are not visible to humans. The first fatal accident of a self-driving car, when an autopiloted Tesla ran into the side of a truck that was not detected by the on-board computer because the white truck could not be distinguished from the white sky background,[51] made it clear that the deployment of autonomous vehicles is ahead of the development of the transportation infrastructure of our society. If the truck side would have carried a coating that reflects a specific IR signal, ideally realized using CLC shells with appropriate pitch, the car could have avoided the fatal mistake.

The ideal location for incorporating IR-reflecting CLC shells for guiding machines that navigate through the city is, in addition to the outsides of the machines themselves, the facades (sides) of the buildings in the city. Indeed, contemporary architects already take advantage of facades in their design, as they commonly have no structural requirement. Many of today's interactive buildings, or buildings displaying information, utilize the facade for this function. By optimizing the materials used for reflections outside the human vision spectrum, there would be little or no negative aesthetic consequences for cityscape and vehicle design. These invisible coatings could revolutionize navigation of unmanned vehicles such as air drones and semi- or fully self-driving cars, adding significantly to the safety of such future technologies.

Interestingly, the same concept applied to building interiors would be just as useful. As modern humans, we spend most of our time indoors, hence we constantly encounter windows, interior walls, and doors. There is thus much reason to explore means of giving these common features of our indoors infrastructure enhanced functions by adding appropriate advanced materials. Although in the media the most commonly discussed class of autonomous vehicles is that of driverless cars occupying outdoor roads, much research is being done also on smaller vehicles that can be used indoors.[52] Such vehicles would profit greatly from a machine-only information landscape provided by CLC shells applied on interior surfaces.

Of course, we can also design large-scale CLC shell coatings to be useful for humans. Interactions in space between infrastructure and humans, mostly defined in the area of wayfinding, have aesthetic, practical, as well as legal impacts. Fire exits must be located on the building exterior and have closed door access at all times. Egress routes must be specified with signage and emergency backup lights. However, by nature of being reserved for emergencies, this information is rarely needed, and the spontaneous response of building occupants in the case of an incident is to exit in the same way in which they entered.[53] Materials that would change appearance in a way as to encourage people to use the appropriate route would be beneficial in addressing this challenge. In fact, the 1993 bombing of the World Trade Center resulted in numerous changes to building code, including but not limited to "Photoluminescent paint on handrails, stair treads, and stair centerline."[54]

Signage in general is a difficult area to adequately implement. While maps help occupants navigate, the 2D floor plan is not always easily understood. Lines on the ground of an airport terminal or large complexes like theme parks can help in navigating space, but have obvious drawbacks in aesthetic designs and labor for implementing and modifying. Here, the increased popularity of augmented reality through common devices such as smartphones appears as a potential solution, but this requires a platform for communicating information about the environment in a way that is unobtrusive to people. Smartphones are since long equipped with a multitude of sensors and cameras, with the latest generation including IR illumination and imaging (used in face recognition). CLC shells could aid significantly in the wayfinding experience, either through directly visible cues (constant or appearing only in the case of an emergency) or as an interface to a smartphone (or other future technology), which on demand would translate invisible IR signage into information tailored for a specific user.

To better understand the application opportunities of CLC shells on large scale, we first briefly summarize how current motion capture technology exploits nondescriminative omnidirectional back reflection, a solution that lends itself well to further advancement using CLC shells. Motion capture technology also serves as an excellent illustration of how a large number of tiny objects can perform functions on macroscopic scale.

3.2.1. Omnidirectional Reflectors in Motion Capture

In the realm of motion capture—digitizing the motion of humans, animals, or objects—the individuals to be tracked carry special markers, reflective balls that shine light back to a source across the full cross section of the ball, yielding the shape of a perfect circle no matter in which direction the ball is found with respect to the source, see **Figure 11**a,b. IR-sensitive cameras are placed around the object to be tracked, each equipped with an IR LED source, and a computer determines the motion by analyzing the images captured by all cameras (facilitated by the circle shape of each signal). Looking at the reflective surface of a motion capture marker in the optical microscope (Figure 11c) we see that it consists of a large number of tiny bead reflectors, each about 20 µm in diameter. It is this combination of many small reflective beads covering a large sphere that allows the angle-independent circle-shape reflection that characterizes these markers, as illustrated in Figure 11d. If one would place the small spheres on a flat area, as in Figure 11e, one would also get large-area reflection over an extended range of angles, but the apparent shape would change with angle, hence the spherical base is more versatile.

This simple idea of reflective beads on a larger sphere is an elegant solution to ensure that a reflector returns the light back to its source regardless of the illumination direction. It is a good basis for making navigation of autonomous vehicles safer. However, if the background shows similar indiscriminate reflectivity, the signal from motion capture markers would be difficult to detect due to insufficient contrast. Moreover, if a very large number of objects are present which all carry reflectors of this type, there is no way to distinguish which reflections come from which object. Finally, motion capture reflectors are not

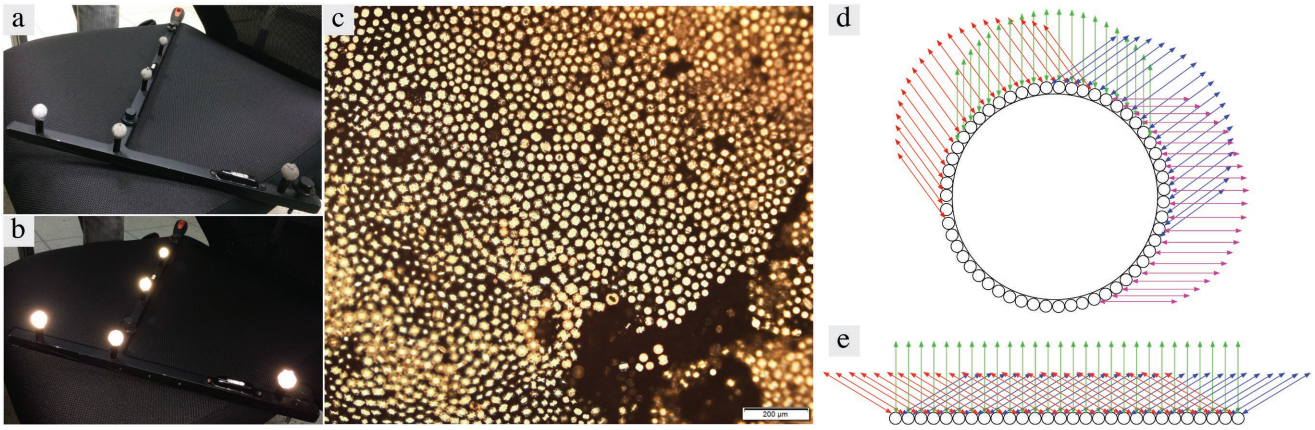

Figure 11. a–c) Markers for motion capture (a,b) are spheres of about 1 cm diameter covered with a very large number of tiny reflective beads (c). This geometry ensures that the full cross section area of the sphere appears as a bright perfect circle when illuminated in any direction, as shown in (b), where a set of motion capture reflector balls is illuminated with a flash at the camera. In (a) no flash was used. The drawings in (d,e) illustrate how light is reflected in circular form by the beads in any direction for the case of the spherical base d), and with an angle-dependent shape for the case of a flat base (e).

invisible, hence their application in buildings or in cityscapes would have a serious aesthetic impact.

3.2.2. Infrastructure for Outdoor Autonomous Vehicles

In order to apply this type of omnidirectional reflector in an autonomous vehicle scenario we must ensure that the reflections are invisible to the human eye and *selective*. CLC shells appear as the ideal candidate to address this challenge, replacing the nondiscriminative reflective beads of present-day motion capture markers. Since we can make CLC shells in many different ways, reflecting left- or right-handed circular polarized light within a band centered around a wavelength that we can tune from several micrometers down to some 100 nm, being complete reflectors or letting in some light to generate patterns from internal reflections, we can combine different types of CLC shells in an effectively infinite number of arrays. This would allow us to distinguish every individual object even in a very busy high-tech future. If we restrict the wavelengths to the IR or the UV ranges this can be done in a way that is invisible to the human eye, in contrast to alternative labeling technologies that can be more disruptive in character.

For assessing the traffic situation, an autonomous car of the future would thus scan not only the visible information, as is the case today, but it could also analyze the reflections upon illumination of the street level landscape with a sequence of IR flashes. This is similar to the motion capture situation, but each flash would have a specific wavelength and polarization matching a certain type of CLC shell. The compound picture arising by superposing the reflected patterns tells the car where there are other vehicles and which types they are. Since the communication is done at the speed of light, the displacement of vehicles between consecutive flashes will be negligible.

On the roads, visible and invisible information could be combined in signage, such as a stop sign at a busy crossing that in the visible spectrum tells the human driver to stop, while simultaneously communicating information to the autonomous car in the IR. The latter data might include the speed limits of the car's road and of those crossing, the angles at which roads cross, how many roads are meeting, and of course the location. While this information is typically included in navigator apps, they rely on functioning GPS or triangulation as well as the right map being loaded into the car's memory; the local environment today provides no information for autonomous vehicles beyond the physical landscape. The information is thus not part of the infrastructure in which the car is driving, but it is up to the owner to purchase this information prior to entering the space or download it in real time, relying on a functioning fast wireless network connection. Moreover, the bidirectional communication opens the possibility of tracking the user. From a safety as well as from a personal integrity point of view there is a clear advantage of having the information freely available at all times, without dependence on electrical power and satellite communication and with no possibility to monitor the individual requesting the information.

How would these coatings be realized and used? A simple but useful design for identifying a vehicle could combine CLC shells of four types, reflecting at two different wavelengths and with left- or right-handed circular polarization. A standardized frame with a specific sequence of the four CLC shell types could be used to identify that this is a coating with the function of a vehicle ID tag, whereas the distribution of CLC shells in the area enclosed by the frame would be unique to the type of vehicle. By suspending CLC shells in a photocurable index matching liquid, the tag would be completed by illuminating the whole tag with UV light. In contrast to the security tags discussed in Section 3.1.1, the matrix would here be cured only after all shells have adopted their equilibrium positions, as in this case we want a standardized pattern.

The design of an individual reflector in the ID tag pattern could be modeled on the motion capture concept, thus a macroscopic transparent sphere that is covered by smaller polymerized CLC shells of the desired type. However, the size of the macroscopic sphere that would give a large enough reflection for the probing car to read the pattern at reasonable distance may be so large that the tag would have an obtrusive extension also in the third dimension. A flat tag design (Figure 11e) may therefore be better, although this would require some image processing for compensating for the angle dependence of the tag pattern. Here the effective frame shape could be used as reference, in order to digitally unskew the pattern as appropriate for the image analysis.

A potential problem are the reflections at wavelengths $\lambda_{\theta\neq 0} < \overline{n}p$ arising for illumination from a direction different from the observation direction, as in Figure 5e. If $\overline{n}p$ is close to the visible range, then oblique reflections will still be visible to humans. A solution may be to coat the tag with a thin layer of material that is opaque to visible light but transparent in the IR window chosen for machine communication. If such a cover is not an option, for instance if the surface must remain transparent in the visible, p should be chosen long enough that all significant oblique reflections are in the IR range. One could also make p so short that all reflections, normal and oblique, are in the UV range, but the probing of tags must then be done with UV light, with obvious risks for unprotected pedestrians, bicyclists, and animals. Future research needs to assess the patterns from IR and UV reflecting CLC shells, with and without coatings of different types, under varying illumination conditions.

In order to read out the information provided by the tags, the autonomous vehicle would need an IR (or UV) imaging equipment capable of filtering out all wavelengths outside the selected communication channel, as well as a switchable circular polarizer optimized for the relevant wavelengths. An advantage of using circular polarization is that noise in the chosen communication channel is linearly polarized or unpolarized, hence it is easy to remove the background by subtracting the right-handed polarized image from the left-handed or vice versa. For illuminating the tags, each vehicle could be equipped with semiconductor IR LEDs or IR lasers such as the VCSELs that are today employed for 3D sensing. Of course, care must be taken that intensities and wavelengths are kept in the realm that is safe for human and animal passersby, even when a large number of autonomous vehicles are operating in a limited space. Another issue to consider for the case of outdoor autonomous vehicles is absorption and scattering of the IR radiation by water in the air (fog, rain, snow, ...) and by deposits on the tags. By

choosing the right wavelength window and by coating tags with antifouling surfaces, thus taking advantage of complementary advanced coatings, these effects can be minimized, although they can never be eliminated entirely. The CLC-shell-based information sharing would thus always be complemented by other techniques, not least the visual image processing that is already in use.

The combination with other techniques is critical also from a fundamental trust point of view, since we need to consider the risk of errors in reading the tags as well as an adversary tampering with the tags. Errors in reading can be detected and corrected by using common procedures for checksums and error correction, like the ones used today for correcting QR code read-out. The problem of detecting potentially misplaced CLC-shell-based tags would best be solved by combining tag reading with image processing. For example, to validate the reliability of a tag saying that an approaching vehicle is a police car, the autonomous vehicle needs to verify that the object has the physical characteristics of a police car. Using two systems in decision making is actually what happens in the brain of humans, where a fast instinctual decision can, in case of need, give space to a slower rational thinking.[55]

3.2.3. Invisible Signage for Indoors Navigation

Autonomous vehicles are likely to play future roles also within buildings as local transport devices. Since GPS works poorly indoors, if at all, a common and simple method for indoor navigation includes following a specific line, similar to how humans follow colored lines in an airport terminal guiding to a specific gate or wing. In order to facilitate the integration of autonomous vehicles indoors, methods such as embedding magnets under flooring (vehicle equipped with Hall effect sensors) to hide the visible line as to not interfere with the architect or designers aesthetic have been demonstrated,[56] although this solution is extremely costly. Another common localization method is the 3D mapping of a space using light detection and ranging (LIDAR). However, with the use of architectural glass in interior space, usually frosted, embossed, or curved, a new set of challenges occurs due to the transmittance of the LIDAR pulse. On the other hand, these properties can be leveraged to communicate information to the robot, for example, by selectively frosting parts of the glass.[57]

IR reflection patterns created by CLC shells incorporated in building interiors would provide indoor autonomous vehicles with an efficient means of navigating at a reasonable cost and with minimum visible impact. Apart from telling the location within the building, such IR signage could give useful just-in-time information about the local surroundings, like the distance before a wall ends or locations of doors that may open into the path being taken, yet without requiring the immediate vicinity of, e.g., RFID tags. Each door could also be labeled with a tag that informs about the type of space behind the door and its occupants.

This type of invisible signage in the walls provides the advantage that it remains functional in case of a power outage in the building since it plays only a passive role. Similar to outdoor autonomous vehicles, the indoor vehicles utilizing the signage would carry their own IR light sources as well as detectors. This autonomy is a crucial advantage in hospitals or military organizations as well as in a rescue or surveillance operation inside a building where the power has been cut for safety reasons. Another area where this is important is deployment in rural areas of developing countries, where electrical power may be unreliable. We expect the communication to be robust even in the case of excessive heating (IR irradiation), e.g., in the case of a fire, thanks to the circular polarization of the reflected light. Since the IR noise (heat) is unpolarized it is cancelled out by substraction of images obtained with right- and left-handed polarizers, respectively. Another alternative is to use ultrashort-pitch CLCs that reflect in the near UV rather than in the IR range, thus operating in a part of the spectrum not affected by heat. For indoors environments without human or animal presence the communication in the UV range would be unproblematic. In other cases, it could be considered a back-up option that normally is not used. Any light-based communication will be obstructed by smoke development, hence the system would only remain in function for areas that are not yet smoke-filled.

3.2.4. Emergency Escape Routes (Abnormal Egress) and Dynamic Wall Signage

So far, our discussion around the use of CLC shells focused on static reflectors, where the LC self-organization is used solely during production, a helix with the pitch chosen for an authentication tag or for a reflector for autonomous vehicle communication being permanently locked in after production via polymerization or templating into a solid replica. This may be inadequate for another aspect of separated visual information, when a special type of information must be communicated to the user—in this case normally human—in the event of an extraordinary situation. From this perspective it becomes interesting to take advantage of the continuous self-organization, and thus tunability of the reflection taking place on a time scale of seconds (p is often strongly dependent on temperature[47]), of a CLC that remains in its fluid state.

The most important and regulated time of egress from a building is in the case of an emergency, such as a fire. Communicating important information like the best direction to move from every point, or providing an easily visible beacon, could aid in the egress during emergencies. To allow CLC shells to adapt their reflective properties for this type of dynamic signage we would need to leave the CLC sufficiently responsive, either by only polymer *stabilizing* the shells lightly rather than polymerizing them completely[15] or by encapsulating a nonpolymerized CLC within a protective sheath that provides mechanical stability. The latter approach has been pioneered by Kim and co-workers, first using a rubber or hydrogel sheath surrounding CLC droplets,[6,17] then surrounding the responsive CLC inside a different CLC that is polymer-stabilized[14] or polymerized. This last solution has the particular advantage that such composite spheres can combine the static signage—here provided by the polymerized outer shell—and the dynamic emergency signage, given by the core of fluid CLC that remains responsive to, e.g., temperature.

The most straightforward application of responsive CLC shells (or droplets) would be in creating signage that starts displaying a visual message if the temperature increases above a certain value, for instance in the case of fire. CLCs have two advantages compared to nonliquid crystalline temperature-responsive pigments. First, the standby state can be colorless transparent, hence the CLC reflectors would be invisible until needed regardless of the background wall color, although a dark background will give the strongest apparent reflection color when activated. While visible reflections from oblique illumination might appear if the stand-by pitch is in the near IR range (Figure 5e), such effects would be absent if the stand-by pitch is instead shorter than visible, in the UV range. Here this is not a safety problem since no UV illumination will ever be used. Second, the color response of CLCs is continuous, spanning the whole visible spectrum from red to violet (or the inverse direction) as the temperature is increased. The latter aspect means that the CLC-based signage could give quantitative information about the temperature, going beyond a simple ON–OFF switch set at a threshold temperature.

Importantly, the CLC response is autonomous, hence the change to visible reflection occurs even if the power is cut, and no electrical wiring needs to be incorporated into the walls. It is also local, providing information to a building occupant of the status of the immediate environment. A problem with the centralized fire alarm systems typically installed in modern hotels and large office buildings is that the occupants do not know *where* the fire has started. They may thus unknowingly be heading toward the fire and even open a door separating them from it. An autonomous coating on walls and doors that is normally invisible, but indicates warning messages in the case of abnormal temperatures on the other side, as could be realized with adequately encapsulated temperature-responsive CLC shells, could thus be an extremely valuable complement to existing alarm systems, with no aesthetic impact, low installation, and zero maintenance cost. This can be used in both the egress of occupants and the entry of emergency responders. Similar to stickers placed on windows for identifying the location of vulnerable people at home (for instance children's rooms), heat-activated visual information can help in guiding emergency responders to vulnerable people trapped in their rooms.

A limitation is that LCs cannot emit light, only reflect it, hence the signage cannot be seen without illumination. However, if daylight reaches the site through windows this is sufficient, and even if occupants find themselves in a windowless part of the building, or the fire starts at night, the typical response today in a situation of failing illumination is to turn on the torch on their mobile phones, allowing them to see the signage during escape. Emergency responders carry their own lights, hence for them this type of heat-activated reflective information is always of value.

An interesting related application is to incorporate an invisible signage that becomes visible in the case of abnormal atmosphere conditions. As mentioned in Section 3.1.2, the omnidirectionality of the color reflected by CLC shells makes a CLC-based sensor more useful than one employing flat CLCs, as the response becomes independent of viewing angle. Moreover, the large surface to volume ratio enhances sensitivity and response speed. If the oxygen sensor described by Han et al.[45] could be optimized to rapidly respond to a critical decrease of oxygen content, its incorporation into the interior walls of a room where compressed or liquid nitrogen, helium, or argon is in use (many research labs) could save lives in case of a gas leakage. For detecting abnormal levels of humidity, dried CNC-based CLCs are of interest as they typically show a reversible color shift from blue to red upon increased humidity.[58]

4. Conclusions and Outlook

Our hope with this paper has been to convey the message that cholesteric liquid crystals, CLCs, have diverse future application potential and that the most interesting options arise when we leave the conventional paradigm of applying them in flat geometries. With the maturity of microfluidic techniques for producing CLC shells fast and consistently, with excellent control of geometrical parameters as well as director alignment, a new path for utilizing liquid crystal self-organization has become available, requiring no alignment layers, patterning of substrates, or other complex additional technologies. The fact that the shells can be rendered long-term stable by polymerization or polymer stabilization, or even templating into an inorganic replica, adds the final critical tool for realistically considering applications of CLC shells.

This is not to say, however, that success should be taken for granted. The rich optics of CLC shells is one of the main selling points for this material, but it also requires much additional effort to reach a mature understanding. Index matching between the CLC and the surrounding phases will be critical for applications aiming to utilize the selective reflection. As outlined above, the utilization of CLC-shell based materials also requires adaptations to the machines and devices that will take advantage of them. While several successful demonstrations of polymerization and polymer stabilization have been presented, this crucial component needs to be further studied. Although cholesteric mixtures have been studied since long, the focus so far on applications near room temperature means that new formulations need to be defined that are tailored for the high temperatures prevalent in the case of a fire. Considering that much of applied liquid crystal research has aimed at bringing the temperatures of desired performance *down*, this is more of a need for a change of mindset than a serious scientific challenge. In order to avoid adverse effects of the continuous phase precursor mixing with the LC and thus affecting its properties prior to curing, the CLC must probably in many cases be completely polymerized or contained in a polymerized protective sheath before being dispersed in the continuous phase. Finally, for true mass production an alternative to the microfluidic production route may need to be developed, although considerable upscaling could be achieved by parallel microfluidic processing.

While these challenges are nontrivial, we are optimistic, based on existing data, that many if not all of them can be overcome. We therefore believe it is fully worthwhile to start considering the use of CLC shells in the novel application scenarios presented here: in secure authentication tags that are practically impossible to clone or simulate, in high resolution pressure sensors that can be incorporated into a robotic skin to give

the robot tactile sensing at its fingertips, in reflective information carriers for guiding autonomous vehicles indoors and outdoors, or in dynamic signage for alerting humans of dangers and/or the best way to escape them. With imagination, an open mindset and with materials optimized for the new applications, the future looks bright and exciting for cholesteric liquid crystals freed from today's constraining rigid flat boundaries.

Acknowledgments

The authors thank J. Noh and V.S.R. Jampani for valuable discussions. Financial support from the European Research Council under the European Union's Seventh Framework Programme (FP/2007-2013)/ERC Grant Agreement no. 648763 (consolidator project INTERACT), University of Luxembourg (project UNIQUE), is gratefully acknowledged. P.B.R. is supported by the INTER-Sequoia project No. 9472655 from the Luxembourg National Research Fund, which is joint with the ANR project SEQUOIA ANR-14-CE28-0030-01. G.L. is supported by "Protocols for Privacy Security Analysis," a pEp Security SA/SnT partnership project.

Conflict of Interest

The authors declare no conflict of interest.

Keywords

cholesteric liquid crystals with spherical topology, functional materials in architecture and design, infrastructure for autonomous vehicles, secure authentication

Received: December 18, 2017
Revised: January 25, 2018
Published online:

[1] A. Aksamija, *Integrating Innovation in Architecture—Design, Methods and Technology for Progressive Practice and Research*, John Wiley & Sons, Chichester, UK **2016**.
[2] Y. Geng, J. Noh, J. P. F. Lagerwall, *Proc. SPIE* **2016**, *9769*, 97690U.
[3] M. Humar, I. Musevic, *Opt. Express* **2010**, *18*, 26995.
[4] Y. Uchida, Y. Takanishi, J. Yamamoto, *Adv. Mater.* **2013**, *25*, 3234.
[5] J. Noh, H.-L. Liang, I. Drevensek-Olenik, J. P. F. Lagerwall, *J. Mater. Chem. C* **2014**, *2*, 806.
[6] S. S. Lee, S. K. Kim, J. C. Won, Y. H. Kim, S. H. Kim, *Angew. Chem., Int. Ed.* **2015**, *54*, 15266.
[7] Y. Geng, J. Noh, I. Drevensek-Olenik, R. Rupp, G. Lenzini, J. P. F. Lagerwall, *Sci. Rep.* **2016**, *6*, 26840.
[8] J. P. F. Lagerwall, G. Scalia, *Curr. Appl. Phys.* **2012**, *12*, 1387.
[9] T. Lopez-Leon, A. Fernandez-Nieves, *Colloid Polym. Sci.* **2011**, *289*, 345.
[10] M. Urbanski, C. G. Reyes, J. Noh, A. G. Sharma, V. S. R. Jampani, J. P. F. Lagerwall, *J. Phys.: Condens. Matter* **2017**, *29*, 133003.
[11] J.-H. Jang, S.-Y. Park, *Sens. Actuators, B* **2017**, *241*, 636.
[12] a) L. E. Aguirre, A. de Oliveira, D. Sec, S. Copar, P. L. Almeida, M. Ravnik, M. H. Godinho, S. Zumer, *Proc. Natl. Acad. Sci. USA* **2016**, *113*, 1174; b) U. Manna, Y. M. Zayas-Gonzalez, R. J. Carlton, F. Caruso, N. L. Abbott, D. M. Lynn, *Angew. Chem., Int. Ed.* **2013**, *52*, 14011; c) I.-H. Lin, D. S. Miller, P. J. Bertics, C. J. Murphy, J. J. de Pablo, N. L. Abbott, *Science* **2011**, *332*, 1297.
[13] H. J. Seo, S. S. Lee, J. Noh, J.-W. Ka, J. C. Won, C. Park, S.-H. Kim, Y. H. Kim, *J. Mater. Chem. C* **2017**, *5*, 7567.
[14] S. S. Lee, H. J. Seo, Y. H. Kim, S. H. Kim, *Adv. Mater.* **2017**, *29*, 1606894.
[15] J. Noh, B. Henx, J. P. F. Lagerwall, *Adv. Mater.* **2016**, *28*, 10170.
[16] S. J. Asshoff, S. Sukas, T. Yamaguchi, C. A. Hommersom, S. Le Gac, N. Katsonis, *Sci. Rep.* **2015**, *5*, 14183.
[17] S. S. Lee, B. Kim, S. K. Kim, J. C. Won, Y. H. Kim, S. H. Kim, *Adv. Mater.* **2015**, *27*, 627.
[18] P.-G. de Gennes, J. Prost, *The Physics of Liquid Crystals*, Clarendon Press, Oxford, UK **1993**.
[19] H. K. Bisoyi, Q. Li, *Acc. Chem. Res.* **2014**, *47*, 3184.
[20] M. Mitov, *Adv. Mater.* **2012**, *24*, 6260.
[21] E. Beltran-Gracia, O. L. Parri, *J. Mater. Chem. C* **2015**, *3*, 11335.
[22] Y. Geng, J. Noh, I. Drevensek-olenik, R. Rupp, J. P. F. Lagerwall, *Liq. Cryst.* **2017**, *44*, 1948.
[23] J. Fan, Y. Li, H. K. Bisoyi, R. S. Zola, D. K. Yang, T. J. Bunning, D. A. Weitz, Q. Li, *Angew. Chem., Int. Ed.* **2015**, *54*, 2160.
[24] H. Khandelwal, A. P. H. J. Schenning, M. G. Debije, *Adv. Energy Mater.* **2017**, *7*, 1602209.
[25] W. D. S. John, W. J. Fritz, Z. J. Lu, D.-K. Yang, *Phys. Rev. E* **1995**, *51*, 1191.
[26] Y. Geng, J.-H. Jang, K.-G. Noh, J. Noh, J. P. F. Lagerwall, S.-Y. Park, *Adv. Opt. Mater.* **2017**, *6*, 1700923.
[27] a) S. N. Fernandes, P. L. Almeida, N. Monge, L. E. Aguirre, D. Reis, C. L. de Oliveira, A. M. Neto, P. Pieranski, M. H. Godinho, *Adv. Mater.* **2017**, *29*, 1603560; b) M. Giese, L. K. Blusch, M. K. Khan, M. J. MacLachlan, *Angew. Chem., Int. Ed.* **2015**, *54*, 2888; c) Y. Nishio, J. Sato, K. Sugimura, *Adv. Polym. Sci.* **2015**, *271*, 241; d) M. Godinho, P. Almeida, J. Figueirinhas, *Materials* **2014**, *7*, 4601; e) D. Klemm, F. Kramer, S. Moritz, T. Lindstrom, M. Ankerfors, D. Gray, A. Dorris, *Angew. Chem., Int. Ed.* **2011**, *50*, 5438; f) J. P. F. Lagerwall, C. Schütz, M. Salajkova, J. Noh, J. H. Park, G. Scalia, L. Bergström, *NPG Asia Mater* **2014**, *6*, e80.
[28] a) J. A. Kelly, M. Giese, K. E. Shopsowitz, W. Y. Hamad, M. J. Maclachlan, *Acc. Chem. Res.* **2014**, *47*, 1088; b) J. A. Kelly, K. E. Shopsowitz, J. M. Ahn, W. Y. Hamad, M. J. MacLachlan, *Langmuir* **2012**, *28*, 17256; c) K. E. Shopsowitz, H. Qi, W. Y. Hamad, M. J. MacLachlan, *Nature* **2010**, *468*, 422; d) K. E. Shopsowitz, J. A. Kelly, W. Y. Hamad, M. J. MacLachlan, *Adv. Funct. Mater.* **2014**, *24*, 327.
[29] K. E. Shopsowitz, A. Stahl, W. Y. Hamad, M. J. MacLachlan, *Angew. Chem., Int. Ed.* **2012**, *51*, 6886.
[30] S. N. Fernandes, Y. Geng, S. Vignolini, B. J. Glover, A. C. Trindade, J. P. Canejo, P. L. Almeida, P. Brogueira, M. H. Godinho, *Macromol. Chem. Phys.* **2013**, *214*, 25.
[31] A. Utada, E. Lorenceau, D. R. Link, P. D. Kaplan, H. A. Stone, D. A. Weitz, *Science* **2005**, *308*, 537.
[32] L.-Y. Chu, A. S. Utada, R. K. Shah, J.-W. Kim, D. A. Weitz, *Angew. Chem., Int. Ed.* **2007**, *46*, 8970.
[33] J. Noh, K. Reguengo De Sousa, J. P. F. Lagerwall, *Soft Matter* **2016**, *12*, 367.
[34] J. Brake, N. Abbott, *Langmuir* **2002**, *18*, 6101.
[35] P. S. Drzaic, *Liquid Crystal Dispersions*, World Scientific, Singapore **1995**.
[36] a) J. H. Kang, S. H. Kim, A. Fernandez-Nieves, E. Reichmanis, *J. Am. Chem. Soc.* **2017**, *139*, 5708; b) J.-G. Kim, S.-Y. Park, *Adv. Opt. Mater.* **2017**, *5*, 1700243; c) K. G. Noh, S. Y. Park, *Mater. Horiz.* **2017**, *1*, 633.
[37] P. Chaudhry, A. Zimmerman, *Protecting Your Intellectual Property Rights*, Springer Science+Business Media, New York **2012**, Ch. 2.
[38] Europol, *2015 Situation Report on Counterfeiting in the European Union*, Office for Harmonization in the Internal Market, The Netherlands **2015**.
[39] Pfizer Global Security, *A Serious Threat to Patient Safety: Counterfeit Pharmaceuticals*, Pfizer Inc., NY **2007**.
[40] B. A. Sullivan, J. M. Wilson, *Trends Organ. Crime* **2017**, *20*, 316.

[41] R. Pappu, B. Recht, J. Taylor, N. Gershenfeld, *Science* **2002**, *297*, 2026.
[42] D. E. Holcomb, W. P. Burleson, K. Fu, *IEEE Trans. Comput.* **2009**, *58*, 1198.
[43] E. Toreini, S. F. Shahandashti, F. Hao, *ACM Trans. Privacy Secur. (TOPS)* **2017**, *20*, 9.
[44] a) M. M. Giraud-Guille, G. Mosser, E. Belamie, *Curr. Opin. Colloid Interface Sci.* **2008**, *13*, 303; b) G. Mosser, A. Anglo, C. Helary, Y. Bouligand, M. M. Giraud-Guille, *Matrix Biol.* **2006**, *25*, 3.
[45] Y. Han, K. Pacheco, C. W. M. Bastiaansen, D. J. Broer, R. P. Sijbesma, *J. Am. Chem. Soc.* **2010**, *132*, 2961.
[46] a) K. D. Cadwell, N. A. Lockwood, B. A. Nellis, M. E. Alf, C. R. Willis, N. L. Abbott, *Sens. Actuators, B* **2007**, *128*, 91; b) J. T. Hunter, N. L. Abbott, *Sens. Actuators, B* **2013**, *183*, 71.
[47] D. J. Mulder, A. P. H. J. Schenning, C. W. M. Bastiaansen, *J. Mater. Chem. C* **2014**, *2*, 6695.
[48] C. Reyes, A. Sharma, J. Lagerwall, *Liq. Cryst.* **2016**, *43*, 1986.
[49] A. Resetic, J. Milavec, B. Zupancic, V. Domenici, B. Zalar, *Nat. Commun.* **2016**, *7*, 13140.
[50] a) T. Horberry, J. Anderson, M. A. Regan, T. J. Triggs, J. Brown, *Accid. Anal. Prev.* **2006**, *38*, 185; b) N. H. Mackworth, *Psychon. Sci.* **1965**, *3*, 67.
[51] A. Davis, Tesla's autopilot has had its first deadly crash, https://www.wired.com/2016/06/teslas-autopilot-first-deadly-crash (accessed: July 2017).
[52] D. Jeon, C.-K. Kim, J. Kim, in *Ubiquitous Robots and Ambient Intelligence*, IEEE, Piscataway, NJ, USA **2015**, p. 512.
[53] J. Tubbs, B. Meacham, *Egress Design Solutions: A Guide to Evacuation and Crowd Management Planning*, John Wiley and Sons, Hoboken, NJ **2007**.
[54] J. D. Averill, D. S. Mileti, R. D. Peacock, E. D. Kuligowski, N. Groner, G. Proulx, P. A. Reneke, H. E. Nelson, *Occupant Behavior, Egress, and Emergency Communications, Federal Building and Fire Safety Investigation of the World Trade Center Disaster*, NIST NCSTAR 1-7, NIST, MD **2005**.
[55] D. Kahneman, *Thinking Fast and Slow*, Farrar, Straus and Giroux, New York **2016**, p. 52.
[56] M. Schwartz, A. Zarzycki, in *Proc. 22nd Int. Conf. Assoc. for Computer-Aided Architectural Design Research in Asia* (Eds: P. Janssen, P. Loh, A. Raonic, M. A. Schnabel), CAADRIA, China **2017**, p. 735.
[57] M. Schwartz, A. Zarzycki, in *Education and Research in Computer Aided Architectural Design in Europe* (Eds: A. Fioravanti, S. Cursi, S. Elahmar, S. Gargaro, G. Loffreda, G. Novembri, A. Trento), ECAADE, Italy **2017**, p. 269.
[58] Y. P. Zhang, V. P. Chodavarapu, A. G. Kirk, M. P. Andrews, *Sens. Actuators, B* **2013**, *176*, 692.